2017

Detecting laminate damage using embedded electrically active plies – An analytical approach

Amany Micheal
The British University in Egypt

Yehia Bahei-El-Din
ybahei@bue.edu.eg

Detecting Laminate Damage Using Embedded Electrically Active Plies – An Analytical Approach

Amany G.B. Micheal* and Yehia A. Bahei-El-Din

Center for Advanced Materials, The British University in Egypt

El-Shorouk City, Egypt

* Corresponding Author, amany.micheal@bue.edu.eg

Keywords

Laminates, bending, averaging models, piezoelectricity.

ABSTRACT

Assessment of damage initiation and progression in composite laminates with embedded electrically active plies is modeled. Utilizing electrically active layers embedded in composite laminates as damage sensors is proposed by several researchers and is mainly assessed experimentally. Sensing damage using embedded electrically active plies is generally preferred over the use of surface mounted PZT wafers since the range of the latter is limited to a very narrow area underneath the surface, while multiple damage mechanisms can generally be found in several plies of the laminate.

The solution presented invokes two levels of analysis. Firstly, on the laminate level, applied membrane loads and/or bending moments induce stresses in the plies according to some distribution factors, which depend on the elastic properties and thickness fractions of the plies. To obtain these factors, the conventional lamination theory is implemented. Secondly, on the ply

level, each unidirectional composite ply, whether electrically active or inactive, is modeled using the Mori-Tanaka averaging model. Both the fiber and matrix stresses are computed and a response in the form of electrical displacement is found in the electrically active plies. Upon damage in certain plies, some eignstresses are applied such that the stress components, which invoke the damage criteria vanish. These eignstresses affect not only the failed plies but also other plies and subsequently the overall behavior of the laminate. Deviations in the electric response of electrically active plies from that found in the undamaged state serves as a damage detector.

This paper outlines a transformation field methodology which implements the above formulation and shows examples for laminates subjected to bending moments. Variation of the electric displacement with the progression of damage is examined in terms of the location of the electroactive ply within the laminate thickness.

1. INTRODUCTION

Coupled behavior of piezoelectric materials such as PZT is now a well-established tool for structure health monitoring. Nowadays, PZT is widely used to build electrically active composites by embedding PZT filaments into a resin matrix to form piezoelectric monolayers rather than using them in their bulk form [1]. Accordingly, the overall mechanical and electrical properties of the electrically active composites must be measured or estimated. This can be found for example in the work of Aboudi [2], Berger et al. [3], Challagulla and Georgiades [4], Chen [5], Hadjiloizi et al. [6, 7], Della and Shu [8], and Kumar and Chakraborty [9]. Sartorato et al. [10, 11] presented a numerical formulation for a finite element shell taking into account a double curvature geometry with some or all layers of piezoelectric composite. The analysis was

performed under dynamic load for natural frequencies and compared with experimental results. Overall moduli of piezoelectric composites with imperfect fiber-matrix adhesion were investigated in the work of Brito-Santana el al. [12] where interface parameters to account for the interface damage were introduced. Tita et al. [13] presented the overall moduli of a smart composite utilizing the RVE approach for both undamaged composite and the composite with imperfect fiber/matrix adhesion. The authors introduced the notion of presenting the interface region in the form of springs with degradable stiffness according to imperfection level.

The use of piezoelectric wafer active sensors, PWAS, for structural health monitoring is on the rise. Many researchers have developed different techniques to utilize surface mounted PWAS for the detection of damage in composites. Among them are Giurgiutiu [14], Giurgiutiu and Soutis [15], Micheal and Bahei-El-Din [16] and Hasan and Muliana [1].

Application on utilizing surface mounted PWAS in detection of the dynamic behavior of a damaged unidirectional composite plate in the form of the change in frequency of the plate is an approach followed by Medeiros et al. [17]. The results were presented both experimentally and numerically. On the other hand, the use of vibration based techniques using PZT sensors to detect any change in stiffness, mass or damping due to inherent damage is found in the work of De Medeiros et al [18] for composite cylinder and its application in automotive components.

Recently, the focus in health monitoring of composite structures has been on embedded sensors. This alleviates the adhesion problems found in the surface mounted ones and relays more reliable information on internal damage. This can be found in the work of Stojic et al. [19] where piezoelectric patches were embedded in concrete structures for the detection of internal cracks. The same approach has been recommended by Lin and Sodano [20] and Qing et al. [21]. The benefits of this methodology can be found in the work of De Medeiros et. al [22] where the

authors present a new damage metric involving the amplitude and the phase under a certain frequency range. Bahei-El-Din and Micheal [23], on the other hand, utilized the electric displacement of PZT fibers to monitor stress concentration for a plate with a central hole. Meanwhile some research has focused on the effect of such inclusions, albeit their small dimensions, on causing stress concentrations [24].

The focus of this paper is on integrating a lamina with electrically active fibers within the layup of a composite laminate to exploit its electric response in detecting the initiation and progression of damage. The paper implements the transformation field analysis [25] to model damage in fibrous laminates. In this approach, damage is modeled by introducing transformation or eign fields to the local regions of the composite plies, which has been affected by damage based on given criteria, such the total stress is evacuated [26]. The paper starts with outlining the laminate governing equations in Section 2, the micromechanical model implemented for a unidirectional, fibrous composite in Section 3, and constitutive equations of piezoelectric materials in Section 4. The damage criterion assigned to the composite constituents is described in Section 5, and is followed in Section 6 by a description of how the electrically active lamina embedded within the laminate layup can serve as a damage detector. Finally, the method is applied to a laminate subjected to external moment in Section 7, and salient conclusions are given in Section 8.

2. LAMINATES

Consider a symmetric laminate of n unidirectional, fibrous composite laminas with a total thickness $2t$ and lamina thickness t_i, $i=1, n$. The laminate global coordinate system is denoted x_j, $j=1,2,3$, where x_1x_2 coincides with mid-plane of the laminate. The lamina principal material

axes are denoted $\bar{x}_k$, $k=1,2,3$, Fig. 1. The laminate is subjected to external membrane forces $\mathcal{N}=[\mathcal{N}_1,\mathcal{N}_2,\mathcal{N}_{12}]$ and bending moments $\mathcal{M}=\left[\mathcal{M}_{11},\mathcal{M}_{22},\mathcal{M}_{12}\right]$. These represent resultants of the lamina in-plane stresses $\hat{\boldsymbol{\sigma}}_i=\left(\sigma_{11},\sigma_{22},\sigma_{12}\right)$, $i=1,\ n$. If in addition the laminas are subjected to transformation stresses $\hat{\boldsymbol{\lambda}}_i=\left(\lambda_{11},\lambda_{22},\lambda_{12}\right),\ i=1,\ n$, which are not removed by unloading of the external loads, membrane forces and bending moments. In analogy with the transformation field analysis developed for inelastic deformations [25, 26], the lamina stresses are found as the superposition of the overall and local effects as [27]:

$$\hat{\boldsymbol{\sigma}}_i(z_i)=\boldsymbol{P}_i\mathcal{N}+\boldsymbol{Q}_i\mathcal{M}+\sum_{j=1,n}\boldsymbol{U}_{ij}\hat{\boldsymbol{\lambda}}_j\ . \tag{1}$$

The coefficient matrices $\boldsymbol{P}_i$ and $\boldsymbol{Q}_i$ denote stress distribution factors for the membrane forces and external moments, respectively, and $\boldsymbol{U}_{ij}$ denotes stress transformation influence functions. They vary point wise along the laminate thickness, and are a function of the laminate geometry and mechanical properties of the laminas [27],

$$\boldsymbol{P}_i=\boldsymbol{L}_i\left(\mathcal{A}'+z_i\mathcal{C}'\right), \tag{2}$$

$$\boldsymbol{Q}_i=\boldsymbol{L}_i\left(\mathcal{B}'+z_i\mathcal{D}'\right), \tag{3}$$

$$\boldsymbol{U}_{ij}=\delta_{ij}\boldsymbol{I}-t_j\boldsymbol{P}_i-\left(t_jz_j\right)\boldsymbol{Q}_i\ . \tag{4}$$

where,

$$\mathcal{A}'=(\boldsymbol{I}-\mathcal{B}'\mathcal{B})\mathcal{A}^{-1},\quad \mathcal{B}'=-\mathcal{A}^{-1}\mathcal{B}\mathcal{D}',\quad \mathcal{C}'=-\mathcal{D}'\mathcal{B}\mathcal{A}^{-1},\quad \mathcal{D}'=[\mathcal{D}-\mathcal{B}\mathcal{A}^{-1}\mathcal{B}]^{-1}, \tag{5}$$

$$\mathcal{A}=\sum_{i=1,n}t_i\boldsymbol{L}_i\ ,\quad \mathcal{B}=\sum_{i=1,n}\left(t_iz_i\right)\boldsymbol{L}_i\ ,\quad \mathcal{D}=\sum_{i=1,n}t_i\left(\frac{1}{12}t_i^2+z_i^2\right)\boldsymbol{L}_i\ . \tag{6}$$

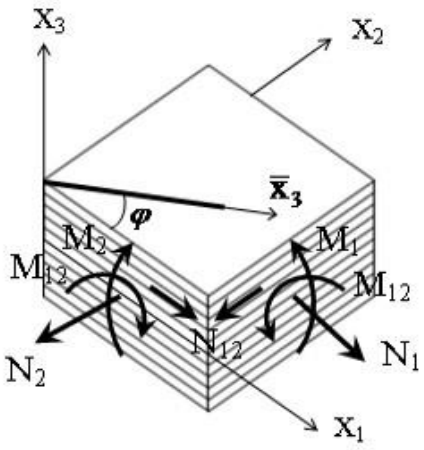

Figure 1. Geometry and loads of a fibrous laminate.

Here, z_i represents the x_3 coordinate of the mid-plane of the ply, and $\boldsymbol{L}_i$ represents the lamina stiffness matrix described in the laminate global coordinate system, and under in-plane stress.

Evaluation of all the above coefficient matrices centers on defining the overall elastic moduli of the individual laminas and hence the stiffness matrix $\boldsymbol{L}_i$. While any micromechanical model of a fibrous composite can be utilized, this is described next in terms of the averaging models.

3. AVERAGING MODEL

Let $\bar{\boldsymbol{\sigma}} = \left(\sigma_{11}, \sigma_{22}, \sigma_{33}, \sigma_{23}, \sigma_{31}, \sigma_{12}\right)$ and $\bar{\boldsymbol{\varepsilon}} = \left(\varepsilon_{11}, \varepsilon_{22}, \varepsilon_{33}, 2\varepsilon_{23}, 2\varepsilon_{31}, 2\varepsilon_{12}\right)$ denote the lamina stress and strain described in the material principal axes, $\bar{x}_k$, $k = 1,2,3$, of a unidirectional fibrous composite, such that $\bar{\boldsymbol{\sigma}} = \bar{\boldsymbol{L}}\bar{\boldsymbol{\varepsilon}}$. The elastic stiffness matrix, $\bar{\boldsymbol{L}}$, can be expressed in terms of elastic moduli of the fiber and matrix and their volume fraction using the Mori-Tanaka model [28]. This centers of Eshelby's solution of an infinitely long cylindrical inclusion embedded in a matrix of a different material [29] to find explicit forms for the fiber and matrix stress and strain

concentration factors [30]. The result was utilized by Chen et al. [31] to determine the Mori-Tanaka overall moduli of a fibrous composite in the following explicit form,

$$p=\frac{2v_f p_m p_f+v_m\left(p_m p_f+p_m^2\right)}{2v_f p_m+v_m\left(p_f+p_m\right)},\quad m=\frac{m_m m_f\left(k_m+2m_m\right)+k_m m_m\left(v_f m_f+v_m m_m\right)}{k_m m_m+\left(k_m+2m_m\right)\left(v_f m_m+v_m m_f\right)}, \tag{7}$$

$$k=\frac{v_f k_f\left(k_m+m_m\right)+v_m k_m\left(k_f+m_m\right)}{v_f\left(k_m+m_m\right)+v_m\left(k_f+m_m\right)},\quad \ell=\frac{v_f \ell_f\left(k_m+m_m\right)+v_m \ell_m\left(k_f+m_m\right)}{v_f\left(k_m+m_m\right)+v_m\left(k_f+m_m\right)}, \tag{8}$$

$$n=v_m n_m+v_f n_f+\left(1-v_f\ell_f-v_m\ell_m\right)\frac{\ell_f-\ell_m}{k_f-k_m}, \tag{9}$$

where k,ℓ,m,n,p are Hill's moduli [32] for a transversely isotropic medium. They are related to the Engineering moduli by

$$k=-\left[1/G_T-4/E_T+4\nu_L^2/E_L\right]^{-1},\quad \ell=2k\nu_L, \tag{10}$$

$$n=E_L+4k\nu_L^2=E_L+\ell^2/k,\quad m=G_T,\quad p=G_L. \tag{11}$$

Here, E_L, G_L, ν_L are longitudinal Young's modulus, shear modulus and Poisson's ratio, and E_T, G_T, $\nu_T=E_T/2G_T-1$ are their transverse counterparts. If $\bar{x}_3$ is the axis of rotational symmetry, the elastic stiffness matrix is written [32]

$$\bar{\boldsymbol{L}}=\begin{bmatrix} 1/E_T & -\nu_L/E_T & -\nu_L/E_L & 0 & 0 & 0\\ & 1/E_T & -\nu_L/E_L & 0 & 0 & 0\\ & & 1/E_L & 0 & 0 & 0\\ & & & 1/G_L & 0 & 0\\ & SYM. & & & 1/G_L & 0\\ & & & & & 1/G_T \end{bmatrix}^{-1}=\begin{bmatrix} (k+m) & (k-m) & \ell & 0 & 0 & 0\\ & (k+m) & \ell & 0 & 0 & 0\\ & & n & 0 & 0 & 0\\ & & & p & 0 & 0\\ & SYM. & & & p & 0\\ & & & & & m \end{bmatrix}. \tag{12}$$

In utilizing eq. (12) in the laminate analysis of Section 2, it is first reduced to relate plane stresses, $\hat{\bar{\boldsymbol{\sigma}}}=\left(\sigma_{22},\sigma_{33},\sigma_{23}\right)$, and their corresponding strain components, $\hat{\bar{\boldsymbol{\varepsilon}}}=\left(\varepsilon_{22},\varepsilon_{33},2\varepsilon_{23}\right)$, and then transformed to the laminate global axes. The result is [33],

$$\hat{\hat{\boldsymbol{L}}} = \frac{1}{k+m}\begin{bmatrix} 4km & 2m\ell & 0 \\ 2m\ell & E_L k + mn & 0 \\ 0 & 0 & p(k+m) \end{bmatrix}, \tag{13}$$

$$\hat{\boldsymbol{L}} = \boldsymbol{N}^{\mathrm{T}} \hat{\hat{\boldsymbol{L}}} \boldsymbol{N}, \tag{14}$$

$$\boldsymbol{N}^{-1} = \begin{bmatrix} \sin^2\varphi & \cos^2\varphi & -\frac{1}{2}\sin 2\varphi \\ \cos^2\varphi & \sin^2\varphi & \frac{1}{2}\sin 2\varphi \\ -\sin 2\varphi & \sin 2\varphi & \cos 2\varphi \end{bmatrix}, \tag{15}$$

where φ is the angle between the $\bar{x}_3$-axis and the x_1-axis, Fig. 1.

4. PEIZOELECTRIC SENSORS

We consider the role of piezoelectric fibers as sensors and quantify the electric displacement $\mathcal{D} = (\mathcal{D}_1, \mathcal{D}_2, \mathcal{D}_3)$ caused by the stress, $\boldsymbol{\sigma} = (\sigma_{11}, \sigma_{22}, \sigma_{33}, \sigma_{23}, \sigma_{31}, \sigma_{12})$, or strain, $\boldsymbol{\varepsilon} = (\varepsilon_{11}, \varepsilon_{22}, \varepsilon_{33}, 2\varepsilon_{23}, 2\varepsilon_{31}, 2\varepsilon_{12})$, as [34]

$$\mathcal{D} = \boldsymbol{d}\boldsymbol{\sigma} = \boldsymbol{e}\boldsymbol{\varepsilon}, \tag{16}$$

where $\boldsymbol{d}$, $\boldsymbol{e}$ are (3x6) matrices of piezoelectric constants. For transverse isotropy with $\bar{x}_3$ the axis of rotational symmetry, $\boldsymbol{d}$, $\boldsymbol{e}$ take the following form [5, 35],

$$\boldsymbol{d}^{\mathrm{T}} = \begin{bmatrix} 0 & 0 & d_{31} \\ 0 & 0 & d_{31} \\ 0 & 0 & d_{33} \\ 0 & d_{15} & 0 \\ d_{15} & 0 & 0 \\ 0 & 0 & 0 \end{bmatrix}, \quad \boldsymbol{e}^{\mathrm{T}} = \begin{bmatrix} 0 & 0 & e_{31} \\ 0 & 0 & e_{31} \\ 0 & 0 & e_{33} \\ 0 & e_{15} & 0 \\ e_{15} & 0 & 0 \\ 0 & 0 & 0 \end{bmatrix}. \tag{17}$$

The piezoelectric constants are related by [28],

$$e_{31} = 2kd_{31} + \ell d_{33}, \quad e_{33} = 2\ell d_{31} + nd_{33}, \quad e_{15} = pd_{15}. \tag{18}$$

5. DAMAGE

Damage in composite laminates is assessed locally within each individual ply in terms of stresses referred to the lamina material principal axes. Under membrane force, $\mathcal{N} = [\mathcal{N}_1, \mathcal{N}_2, \mathcal{N}_{12}]$, bending moment, $\mathcal{M} = \left[\mathcal{M}_{11}, \mathcal{M}_{22}, \mathcal{M}_{12}\right]$, and ply in-plane transformation stress $\hat{\boldsymbol{\lambda}}_i = \left(\lambda_{11}, \lambda_{22}, \lambda_{12}\right)$, $i = 1, n$, the lamina stresses, which vary point-wise within the lamina thickness, $\boldsymbol{\sigma}_i(z_i)$, are given by eq. (1). The average lamina stress is then found as

$$\hat{\boldsymbol{\sigma}}_i = \frac{1}{t_i} \int_{z_i - t_i/2}^{z_i + t_i/2} \hat{\boldsymbol{\sigma}}(z) dz, \tag{19}$$

where, t_i is the lamina thickness and z_i is the x_3 coordinate of the mid-plane of the ply measured from the mid-plane of the laminate. These can be transformed into the lamina material principal axes, $\overline{x}_k$, $k = 1,3$, as $\hat{\bar{\boldsymbol{\sigma}}}_i = \boldsymbol{R}_i \hat{\boldsymbol{\sigma}}_i$, where the stress transformation matrix is given by transpose of the matrix shown in eq. (15) [33].

With the full stress vector of the lamina now available in the material principal axes as $\bar{\boldsymbol{\sigma}} = \left(0, \sigma_{22}, \sigma_{33}, \sigma_{23}, 0, 0\right)$, the average stresses in the fiber and matrix can be found, in the presence of phase eigen stresses, as [25]

$$\boldsymbol{\sigma}_r = \boldsymbol{B}_r \bar{\boldsymbol{\sigma}} + \sum_{s=f,m} \boldsymbol{F}_{rs} \boldsymbol{\lambda}_s \ , \quad r = f, m. \tag{20}$$

Here, $\boldsymbol{B}_r$ is stress concentration factor and $\boldsymbol{F}_{rs}$ is stress transformation factor. For averaging models of a fibrous composite, they are given by [26],

$$\boldsymbol{B}_r = \left(\boldsymbol{M}_r - \boldsymbol{M}_s\right)^{-1} \left(\bar{\boldsymbol{M}} - \boldsymbol{M}_s\right) \Big/ \mathrm{v}_r \ , \quad r, s = f, m, \tag{21}$$

$$\boldsymbol{F}_{rf} = \left(\boldsymbol{I} - \boldsymbol{B}_r\right)\left(\boldsymbol{M}_f - \boldsymbol{M}_m\right)^{-1} \boldsymbol{M}_f \ , \quad \boldsymbol{F}_{rm} = -\left(\boldsymbol{I} - \boldsymbol{B}_r\right)\left(\boldsymbol{M}_f - \boldsymbol{M}_m\right)^{-1} \boldsymbol{M}_m \ , \quad r = f, m. \tag{22}$$

where $\bar{\boldsymbol{M}} = \boldsymbol{L}^{-1}$ is overall compliance of the lamina.

The effect of damage on the overall response is effectively in releasing local stresses, which meet certain criteria. This is treated by introducing auxiliary eigen stresses in the fiber and/or the matrix to evacuate the affected stresses [36]. The failure criteria employed by Bahei-El-Din and Botrous [36] for averaging models are utilized. The matrix may fail under tensile or compressive stresses when the ultimate strength magnitudes, $\sigma_{uT}^{(m)}$, $\sigma_{uC}^{(m)}$, are exceeded by the average normal stresses, while the fiber fails under tension only axially if its ultimate strength $\sigma_{uT}^{(f)}$ is exceeded. In this case, the onset of failure is given by,

$$\bar{\sigma}_{ii}^{(m)} = \sigma_{uT}^{(m)} \text{ if } \bar{\sigma}_{ii}^{(m)} > 0, \ \left|\bar{\sigma}_{ii}^{(m)}\right| = \sigma_{uC}^{(m)} \text{ if } \bar{\sigma}_{ii}^{(m)} < 0, \ i = 1,3 \tag{23}$$

$$\bar{\sigma}_{33}^{(f)} = \sigma_{uT}^{(f)} \text{ if } \bar{\sigma}_{ii}^{(f)} > 0. \tag{24}$$

The matrix may also exhibit failure by slip on transverse or longitudinal planes under shear stresses. Considering friction, the failure criteria can be written, respectively, as [36],

$$\tfrac{1}{2}\left|\bar{\sigma}_{11}^{m} - \bar{\sigma}_{22}^{m}\right| + \tfrac{1}{2}\eta_T \left\langle \bar{\sigma}_{11}^{m} + \bar{\sigma}_{22}^{m} \right\rangle = \tau_u^m, \tag{25}$$

$$\bar{\sigma}_{13}^{m} + \eta_L \left\langle \bar{\sigma}_{22}^{m} \right\rangle = \tau_u^m, \tag{26}$$

where η_T and η_L are coefficients of friction for slip in the transverse and longitudinal planes, respectively, $\langle x \rangle = x$ if $x < 0$, $\langle x \rangle = 0$ if $x \geq 0$, and τ_u^m is ultimate shear strength of the matrix.

6. EXPLOITING ELECTRICALLY ACTIVE PLIES IN SENSING DAMAGE

In the absence of electric load, the electric displacement caused in a piezoelectric fiber is a function of the stress sustained, eq. (16). The latter is generally affected by the constraints imposed on the fiber due to embedment in another medium, e.g. a polymer matrix, and/or

bonding to other plies in a laminated construction. The effect of damage in such a laminated construction is to relax the constraints imposed on the piezoelectric fiber, and this leads to a change in the electric displacement generated and serves as a signal for damage. In the transformation field approach described Section 5, damage is reflected by the introduction of an auxiliary eigen stress field to modify the stress states, which satisfy the underlying damage criteria. These cause local stresses in the plies of a laminated construction and hence affect the electric displacement of the active fibers.

This is illustrated in a symmetric laminated plate subjected to an external moment $\mathcal{M}_{11}$, Fig. 1. The laminate consists of 50 glass/DY063-epoxy, fibrous composite plies, which are identical in properties and thickness, and reinforced at 55% by volume. The laminate layup is $\left([0]_9/[\pm 45]_{12}/[90]_4\right)_s$, and the total thickness is 25 mm. Mechanical properties of the fiber and matrix are given in Table 1 together with the damage parameters utilized in eqs. (23)-(26).

Table 1 Mechanical properties of phases

Material	E (GPa)	ν	σ_{uT} (MPa)	σ_{uT} (MPa)	τ_u (MPa)	η_T	η_L
DY063 Epoxy	3.35	0.35	31.72	115	46.36	0.268	0.268
PZT-5A [28]	60	0.34	---	---	----	----	----
Glass Fiber	73	0.21	1900	----	----	----	----

An electrically active ply is embedded within the laminate at different locations and utilized as an interrogating medium for damage. The active ply is comprised of PZT-5A fibers embedded in a DY063 epoxy matrix at volume content of 0.55. Mechanical properties of the fiber are listed in Table 1, and the piezoelectric constants, eqs. (16), (17), are [35] $d_{31} = -171$

$\text{x}10^{-12}$ (m/V), $d_{33} = 347$, $d_{51} = 584$. If half the laminate thickness is denoted by t, the electrically active ply is embedded within the laminate at four locations with 'z' coordinate, measured from the mid-plane, of $\pm t/2$, $\pm t/4$, Fig. 2.

A benchmark problem where the previously introduced 50 plies laminate with no embedded electrically active plies under tension in x_1 direction is investigated. The analysis shows that failure in the 90^o plies occurs first due to matrix damage in axial local direction at overall stress 160 MPa. As the applied stress increases, other failure mechanisms are triggered in other plies. For overall stress of 240 MPa the matrix in the upper and lower 0^o plies fail in the transverse direction and in axial direction for the upper and lower ±45^o plies at the same stress.

To investigate the effectiveness of embedding an electrically active ply in the 50 plies laminate in detecting damage, a bending moment, $\mathcal{M}_{11} = 120$ kN.m/m is applied in six equal increments. At each loading step, all inactive composite plies are checked against the failure criteria given in Section 5 while the active one is assumed undamaged throughout the whole exercise. In any case, the onset of damage occurs in the lower-most plies (Fig. 2) due to axial tensile failure of the matrix (eq. 23) under applied bending moment of 40 kN.m/m. Damage progresses with the increase of applied external moment. The damage progression scheme differs in nature and source with the location of the electrically active ply due to the effect of its stiffness on the distribution of stresses among the plies.

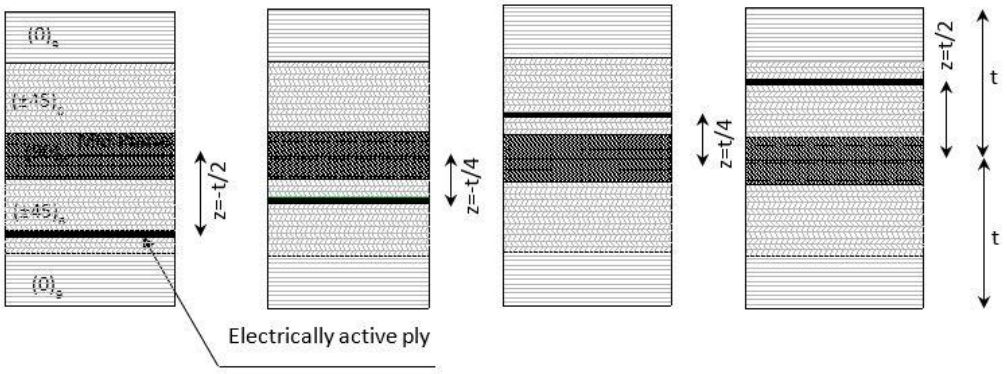

Figure 2. Laminate layup showing different locations of electrically active ply.

Elevating the external moment causes tensile failure in the fiber of the lower-most 0^o plies, and leads to damage progression into other plies. This mechanism is found to occur regardless of the location of the active ply within the laminate. Figures 3 and 4 show progression of failure for active plies located at $z = \pm t/2$ for an external moment of 80 and 100 kN.m/m. Figures 5 and 6 show damage progression at same magnitudes of external moments for active ply located at $z = \pm t/4$. In the legend, failure of the matrix or fiber is denoted. Tables 2 and 3 show the specific failure criteria that is satisfied for both fiber and matrix in every ply. In particular, Table 2 shows the satisfied failure criteria for a laminate with active ply at $z = +t/2$ under external moment of 80 kN.m/m while Table 3 shows the satisfied criteria for the same laminate at external moment of 100 kN.m/m. We note that plies below the neutral axis (NA) shown in Figs. 3-6 are subjected to tensile stresses while those above the NA are subjected to compressive stresses. We also note that while compressive failure of the fiber is expected in the upper most plies, it has been suppressed in this application since it may involve buckling.

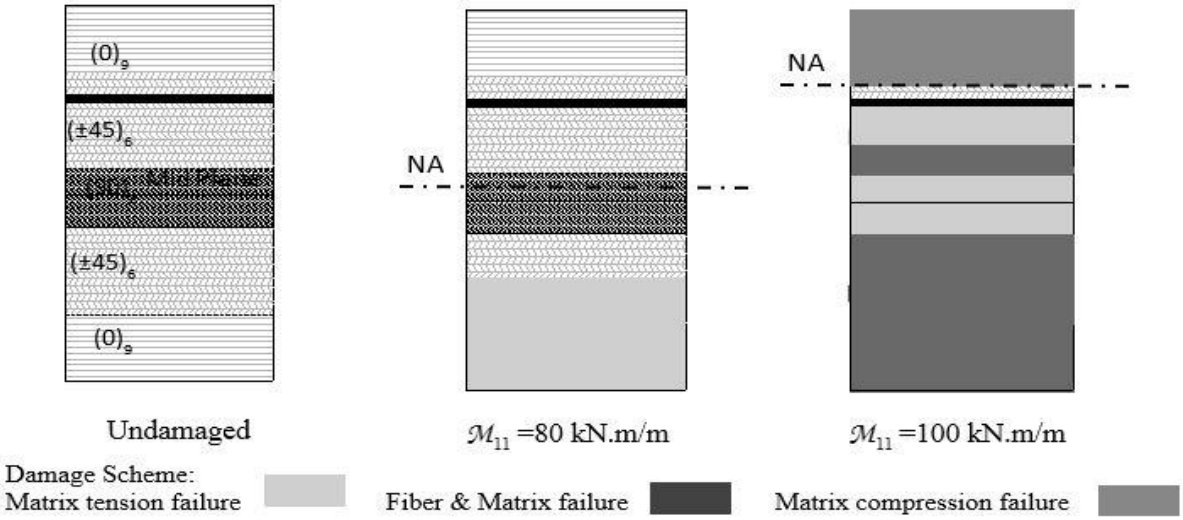

Figure 3. Damage scheme of a fibrous laminate with electrically active ply at z = $+t/2$ under bending moment $\mathcal{M}_{11}$ = 80, 100 kN.m/m.

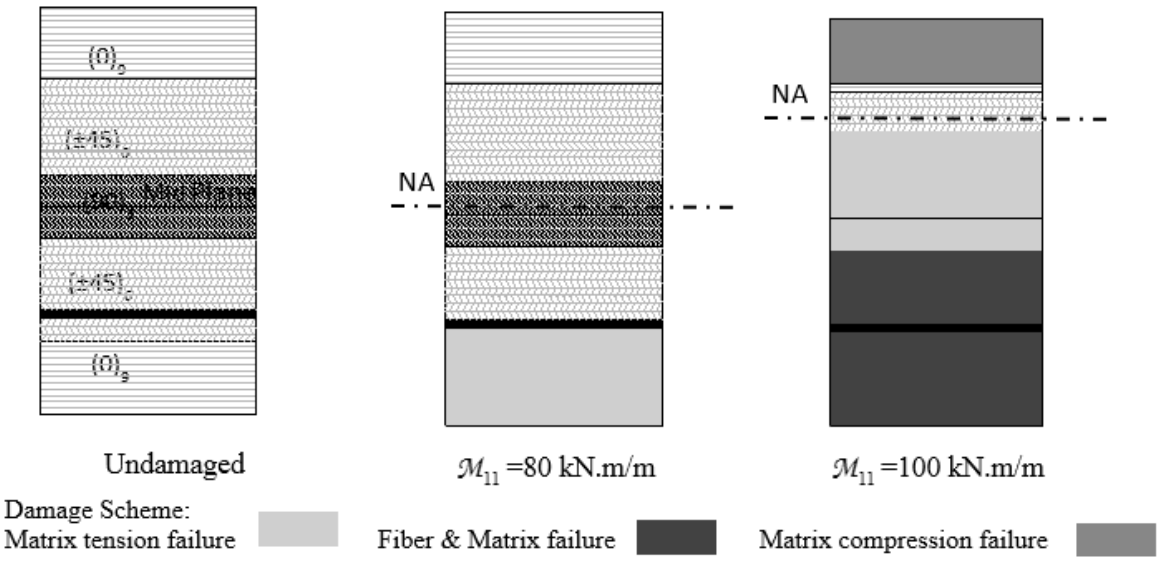

Figure 4. Damage scheme of a fibrous laminate with electrically active ply at z = $-t/2$ under bending moment $\mathcal{M}_{11}$ = 80, 100 kN.m/m.

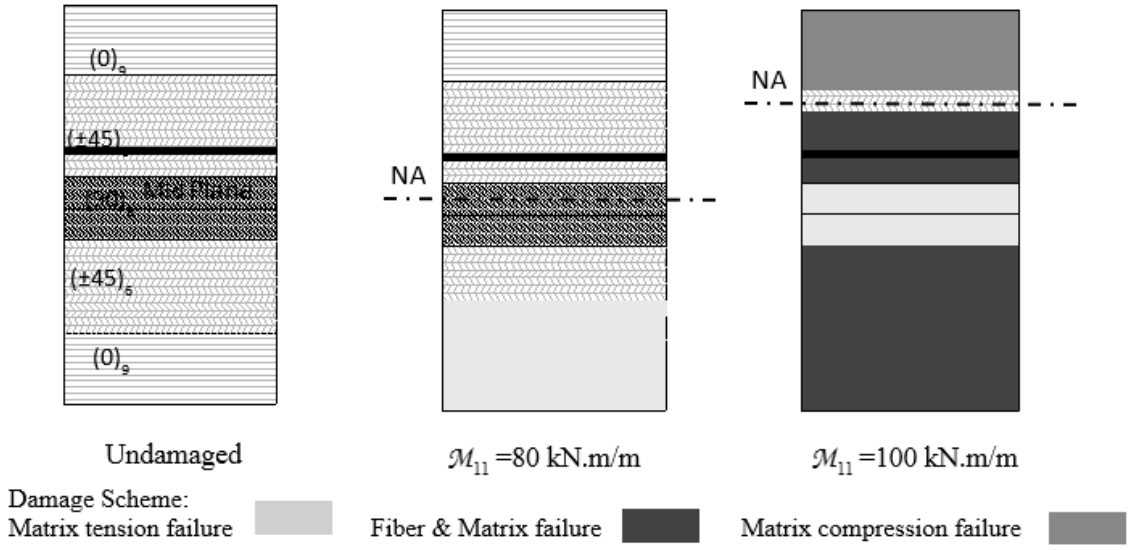

Figure 5. Damage scheme of a fibrous laminate with electrically active ply at z = $+t/4$ under bending moment $\mathcal{M}_{11}$ = 80, 100 kN.m/m.

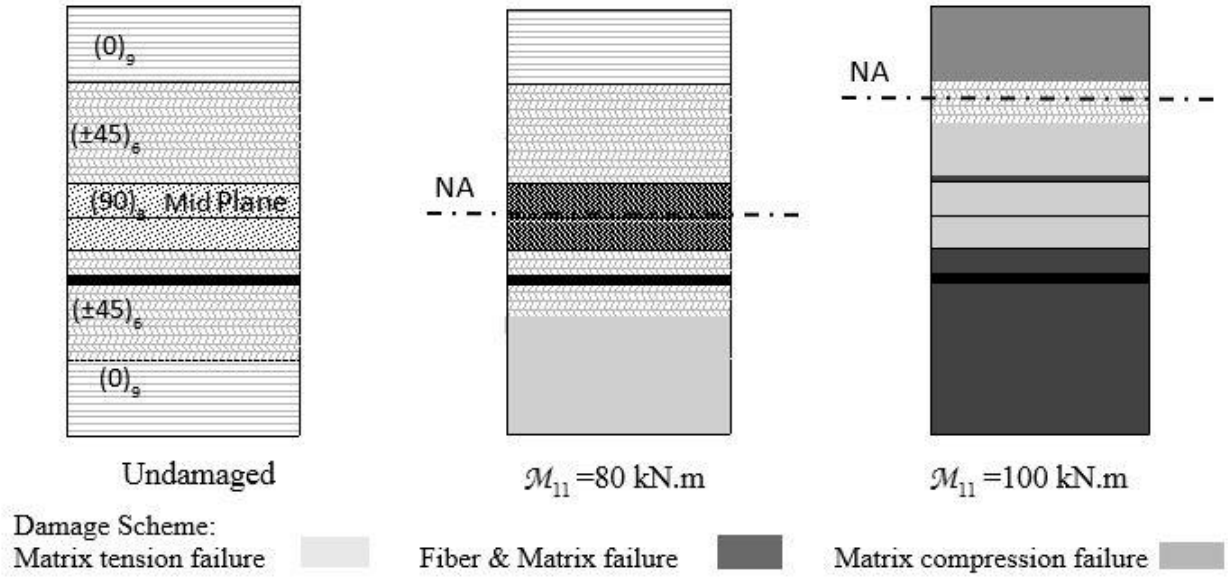

Figure 6. Damage scheme of a fibrous laminate with electrically active ply at $z = -t/4$ under bending moment $\mathcal{M}_{11}$ = 80, 100 kN.m/m.

Table 2. Damage scheme of laminate with an electrically active ply at $z = +t/2$ under $\mathcal{M}_{11}$ = 80 kN.m/m.

Ply	Matrix Tension		Matrix Compression		Matrix Shear		Fiber Axial Tension
	Axial	Transverse	Axial	Transverse	Longitudinal	Transverse	
$(0)_9$							
$(\pm45)_6$							
$(90)_8$							
$(\pm45)_3$							
$(\pm45)_2$							
(-45)							
(+45)							
$(0)_9$							

Table 3. Damage scheme of laminate with an electrically active ply at $z = +t/2$ under $\mathcal{M}_{11}$ = 100 kN.m/m.

Ply	Matrix Tension		Matrix Compression		Matrix Shear		Fiber Axial Tension
	Axial	Transverse	Axial	Transverse	Longitudinal	Transverse	
$(0)_5$							
$(0)_4$							
(+45)							
(-45)							
(+45)							
(-45)							
$(\pm45)_2$							
$(\pm45)_2$							
$(90)_8$							
$(\pm45)_2$							
(-45)							
(+45)							
(-45)							
(+45)							
(-45)							
(+45)							
(-45)							
(+45)							
$(0)_9$							

To investigate the lack of the damaged plies constraint on the electrical response of the active plies, the electrical displacement of the electrically active fibers is plotted versus the applied external moment for different ply locations as shown in Figs. 7 and 8. It is clear that at any loading step associated with a specific failure mode in any ply, the electrically active fibers electric displacement exhibits sudden increase. The effect of the damage status at external moment of 100 kN.m/m on the electric displacement of the active plies is reflected into a drastic increase in D_3.

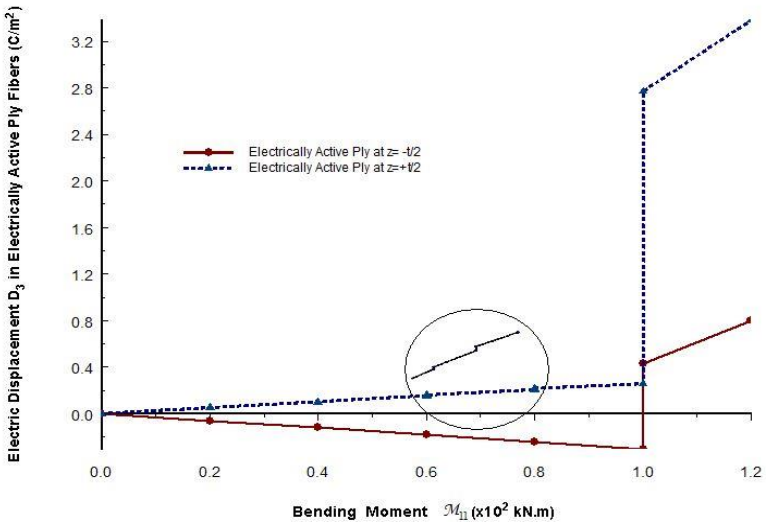

Figure 7. Electric displacement of active ply at $z = \pm t/2$.

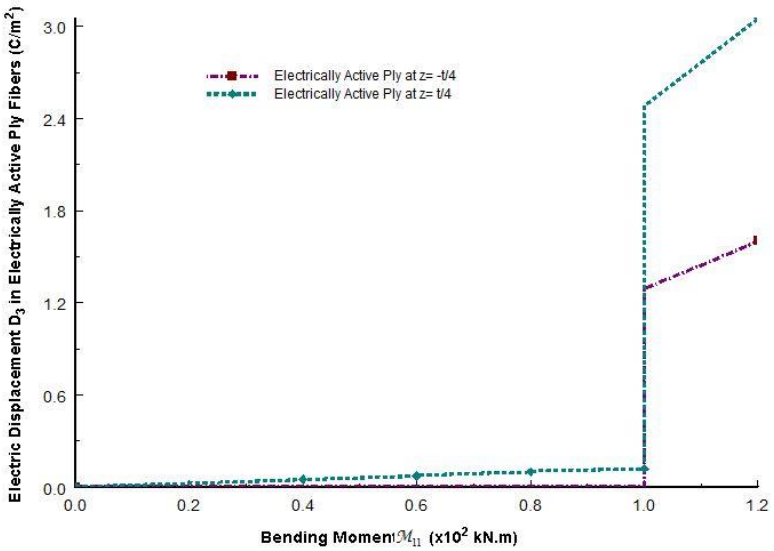

Figure 8. Electric displacement of active ply at $z = \pm t/4$.

The effect of the location of the active plies on its response to failure in terms of electrical displacement D_3 is shown in Fig. 9. It can be easily seen that the effect of damage on the electrical response of active plies is highly pronounced in the location of $z = -t/2$. This can be attributed to the proximity of the active ply to the most damaged portion of the laminate.

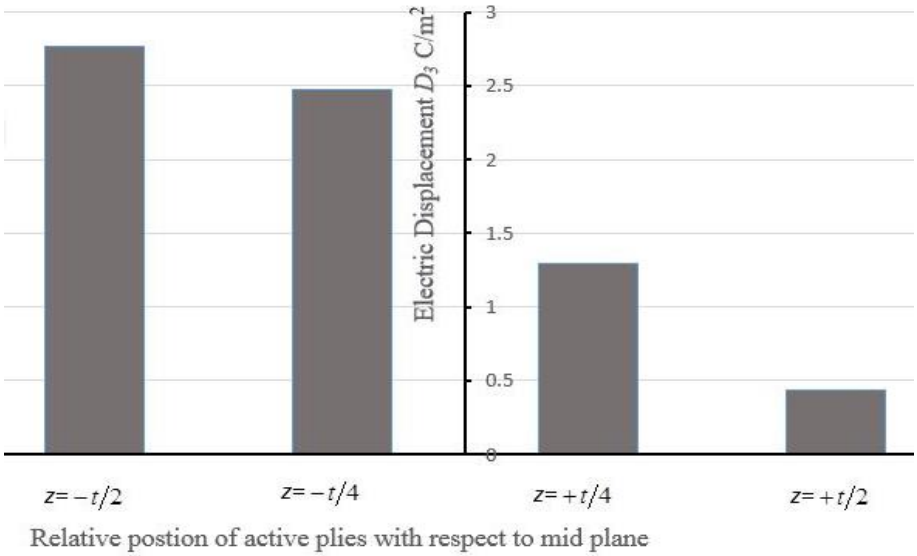

Figure 9. Electric displacement of active ply at different locations under bending moment $\mathcal{M}_{11}$ =100 kN.m/m.

The stress σ_{11} distribution through the laminate thickness of this particular location at external moment of 100 kN.m/m is presented in Fig. 10. It can be deduced that the 0º plies in the lower half of the laminate do not contribute in laminate stiffness at this loading stage due to failure of both constituents. As damage propagates, the neutral axis gets upward and the compression stress in the most upper plies increases. The compression stress σ_{11} of the surface 0º plies; i.e. in fiber axial direction, in case of $z = -t/2$ attains a value of 2500 MPa yet the ply contributes to load bearing due to the assumption that the fibers will not fail in compression as stated earlier.

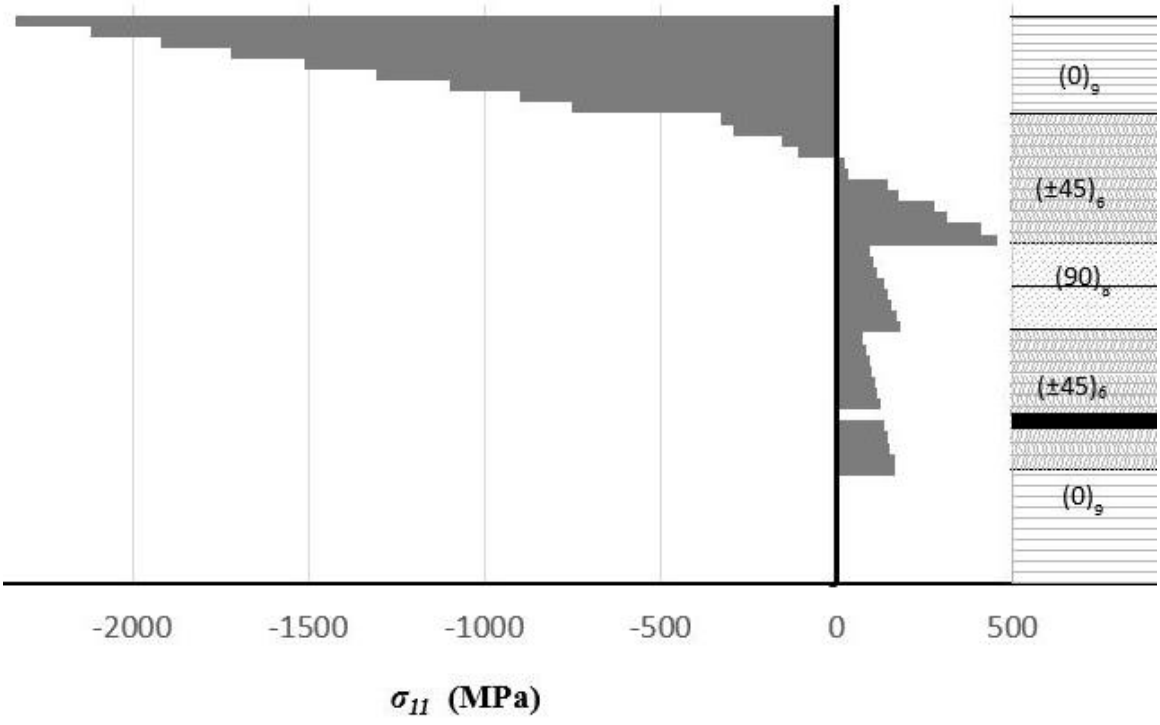

Figure 10. Stress distribution for a fibrous composite laminate with electrically active ply at $z = -t/2$ under bending moment $\mathcal{M}_{11}$ = 100 kN.m/m.

7. CONCLUSIONS

Embedment of electrically active plies within conventional composite laminate serves as an interrogating tool for the laminate integrity. The abrupt changes in the electric displacement of the active fibers reflect the onset and subsequent progressive inherent damage in the laminate. As more laminas lose their ability to share in load bearing, the electrically active ply fibers stresses increase and subsequently the electric response increases in terms of higher values of the electric displacement. The location of the active ply within conventional composite plies has a significant effect on utilizing it as an alarming agent. Choosing the location of the active ply depends primarily on the type of loading and the laminate layup. The transformation field analysis is utilized to deal with plies damage while the conventional laminate theory is implemented to distribute the applied loads among plies according to their stiffness. Certain failure criteria are set, which when satisfied some eignstresses are applied on the laminate to evacuate the failed stresses. The effect of failure of any set of plies on the stress distribution along the laminate thickness was also studied.

REFERENCES

[1] Hasan Z, Muliana A. Failure and deformation analysis of smart laminated composite. Mechanics of Composite Materials 2012; 48: 391-404.

[2] Aboudi J. Micromechanical analysis of fully coupled electro-magneto-thermo-elastic multiphase composites. Smart Materials and Structures 2001; 10: 867-877.

[3] Berger H, Kari S, Gabbert U, Rodriguez-Ramos R, Guinovart R, Otero JA, Bravo-Castillero J. An Analytical and Numerical Approach for Calculating Effective Material

Coefficients of Piezoelectric Fiber Composites. International Journal of Solids and Structures 2005; 42:5692-5714.

[4] Challagulla KS, Georgiades AV. Micromechanical analysis of magneto-electro-thermo-elastic composite materials with applications to multilayered structures. International Journal of Engineering Science 2011; 49: 85-104.

[5] Chen T. Micromechanical Estimates of the Overall Thermoelectroelstic Moduli of Multiphase Fibrous Composites. Int. J. Solids and Structures 1994; 31(22):3099-3111.

[6] Hadjiloizi DA, Georgiades AV, Kalamkarov AL, Jothi S. Micromechanical Modeling of Piezo-Magneto-Thermo-Elastic Composite Structures: Part II – Applications. European Journal of Mechanics 2012, A/Solids, DOI: 10.1016/j.euromechsol.2012.11.003.

[7] Hadjiloizi DA, Georgiades AV, Kalamkarov AL, Jothi S. Micromechanical Modeling of Piezo-Magneto-Thermo-Elastic Composite Structures: Part I – Theory. European Journal of Mechanics 2013, A/Solids, DOI: 10.1016/j.euromechsol.2012.11.009.

[8] Della CN, Shu D. On the Performance of 1-3 Piezoelectric Composites with a Passive and Active Matrix. Sensors and Actuators A 2007; 140:200-2060.

[9] Kumar A, Chakraborty D. Effective Properties of Thermo-Electro-Mechanically Coupled Piezoelectric Fiber Reinforced Composites. Material & Design 2009; 30(4): 1216-1222.

[10] Sartorato M, De Medeiros R, Tita V. A finite element formulation for smart piezoelectric composite shells: Mathematical formulation, computational analysis and experimental evaluation. Composite Structures 2015;127 : 185 - 198.

[11] Sartorato M, De Medeiros R, Vandepitte D, Tita V. Computational model for supporting SHM systems design: Damage identification via numerical analyses. Mechanical Systems and Signal Processing 2017; 84 : 445 – 461.

[12] Brito-Santana H, De Medeiros R, Rodriguez-Ramos R, Tita V. Different interface models for calculating the effective properties in piezoelectric composite materials with imperfect fiber-matrix adhesion. Composite Structures 2016; 151 :70 - 80.

[13] Tita V, Medeiros R, Marques F D, Moreno ME. Effective properties evaluation for smart composite materials with imperfect fiber-matrix adhesion. Journal of Composite Materials 2015; 49: 3683-3701.

[14] Giurgiutiu V. Predictive methodologies for the design lamb-wave piezoelectric wafer active sensors for structure health monitoring, damage detection and failure prevention. In: NSF Engineering Research and Innovation Conference, Honolulu, Hawaii, 22-25 June 2009.

[15] Giurgiutiu V, Soutis C. Enhanced composite integrity through structural health monitoring. Appl Compos Mater 2012; 19(5) : 813-829.

[16] Micheal AGB, Bahei-El-Din YA. Finite element simulation of PZT-aided interrogation of composite laminates exhibiting damage. In: Proceedings of the ASME 2016 International Mechanical Engineering Congress & Exposition. ASME 2016 IMECE, Phoenix, Arizona, 11-17 November 2016.

[17] De Medeiros R, Sartorato M, Vandepitte D, Tita V. A comparative assessment of different frequency based damage detection in unidirectional composite plates using MFC sensors. Journal of Sound and Vibration 2016; 383 : 171 - 190.

[18] Medeiros R, Ribeiro M L, Tita V. Computational methodology of damage detection on composite cylinders: structural health monitoring for automotive components. Int. J. of Automotive Composites 2014;1 : 112 - 128.

[19] Stojic D, Nestorovic T, Markovic N. The application of piezoelectric transducers in the structure health monitoring of reinforced concrete structures. In: 12th International

Multidisciplinary Scientific GeoConference and Expo-Modern Management of Mine Producing, Geology and Environmental Protection 2012; 2: 641-647.

[20] Lin Y, Sodano H A. Concept and model of a piezoelectric structural fiber for multifunctional composites. Composite Science and Technology 2008; 68: 1911-1918.

[21] Qing XP, Wang Y, Gao L, Kumar A. Distributed multifunctional sensor network for composite structural state sensing. In: Proceedings of SPIE - The International Society for Optical Engineering 2012; 8345, art. no. 83453O.

[22] De Medeiros R, Lopes H M R, Guedes R M, Vaz M A P, Vandepitte D, Tita, V. A New Methodology for Structural Health Monitoring Applications. Procedia Engineering 2015; 114: 54 – 61.

[23] Bahei-El-Din YA, Micheal AG. Multiscale analysis of multifunctional composite structures. In: Proceedings of the ASME 2013 International Mechanical Engineering Congress & Exposition. ASME 2013 IMECE, San Diego, California, 13-21 November 2013.

[24] Ghezzo F, Huang Y, Nemat-Nasser S. Onset of resin micro-cracks in unidirectional glass fiber laminates with integrated SHM sensors: experimental results. Structural Health Monitoring 2009; 8 : 477-491.

[25] Dvorak GJ. Transformation field analysis of inelastic composite, Proceedings of the Royal Society London 1992; A437: 311-327.

[26] Dvorak GJ, Benveniste Y. On transformation strains and uniform fields in multiphase elastic Media. Proc. R. Soc. London 1992; A 437: 291–310.

[27] Bahei-El-Din YA, Khire R, Hajela P. Multiscale transformation field analysis of progressive damage in fibrous laminates. International Journal for Multiscale Computational Engineering 2010; 8(1): 69-80.

[28] Mori T, Tanaka K. Average stress in matrix and average elastic energy of materials with misfitting Inclusions. Acta Metallurgica 1973; 21: 571-574.

[29] Eshelby JD. The determination of the elastic field of an ellipsoidal inclusion, and related problems. Proceedings of the Royal Society London 1957; A241: 376-396.

[30] Benveniste Y. A new approach to the application of Mori–Tanaka theory in composite materials. Mechanics of Materials 1987; 6: 147–157.

[31] Chen T, Dvorak GJ, Benveniste Y. Mori–Tanaka estimates of the overall elastic moduli of certain composite materials. Journal of Applied Mechanics 1992, 59: 539–546.

[32] Hill R. Theory of mechanical properties of fibrestrengthened materials: I. Elastic behaviour. Journal of the Mechanics and Physics of Solids 1964; 12: 199–212.

[33] Bahei-El-Din YA. Uniform fields, yielding, and thermal hardening in fibrous composite laminates. International Journal of Plasticity 1992; 8: 867-892.

[34] Nye J F. Physical Properties of Crystals. Oxford University Press, London, 1985.

[35] Bahei-El-Din YA. Modeling electromechanical coupling in woven composites exhibiting damage. In : Proceedings of IMECHE, Part G: J Aerospace Engineering 2009; 223: 485-495.

[36] Bahei-El-Din YA, Botrous AG. Analysis of progressive fiber debonding in elastic laminates. International Journal of Solids and Structures 2003; 40(25): 7035-7053.